International Applied Mechanics, Vol. 48, No. 5, September, 2012

MODELING A CRACK WITH A FRACTURE PROCESS ZONE IN A NONLINEAR ELASTIC BODY

A. A. Kaminsky and E. E. Kurchakov

The role of the fracture process zone near the tip of a mode I crack in a nonlinear elastic body is studied. A boundary-value problem is solved numerically to examine the effect of the fracture process zone on the size and shape of the nonlinear zone near the crack tip

Keywords: nonlinear elastic body, mode I crack, fracture process zone, nonlinear zone

Introduction. As the experiments [5, 6, 11] show, fracture occurs within a local region (fracture process zone) near the crack tip where submicrocracks occur due to very high stresses. The parameters of this zone depend on the properties of the body and the magnitude of the external load.

Because of the inadequate understanding of fracture behavior, fracture process zone models are widely used [10]. The fracture process zone is commonly shorter than the crack and is often located on its continuation. Therefore, if the external load is tensile, the fracture process zone is usually modeled, developing the Leonov–Panasyuk model [7], by a cut with stresses applied to its faces.

The experiments [5, 6, 11] show that the fracture process zone occurs within a nonlinear (deformation) zone near the crack tip. This zone affects both the crack opening displacement [13] and the nonlinear zone.

The present paper examines the effect of the fracture process zone on the nonlinear zone. As in [13], we will use the model [4, 11] that assumes that the length of the fracture process zone (and, hence, the cut) remains constant under increasing external load. It is the stresses applied to the faces of the cut that change. They are assumed to be finite and continuous in the fracture process and nonlinear zones [1, 2, 7, 8] and determined by solving a boundary-value problem. Using this model, we will study the role of the fracture process zone near the crack tip in a nonlinear elastic body in a generalized plane stress state. Strains are assumed small. The boundary-value problem is formulated in terms of the displacement components. By solving a boundary-value problem numerically, we will describe how the fracture process zone affects the size and shape of the nonlinear zone.

1. Preliminaries. To formulate the boundary-value problem, we will use constitutive equations relating the stress (***S***) and strain (***D***) tensors.

1.1. Constitutive Equations. We will use the following linear tensor constitutive equations [13]:

$$S^{\alpha\beta} = \frac{1}{\sigma}\left[g^{\alpha\gamma} g^{\beta\delta} D_{\gamma\delta} - \frac{\rho \mathrm{E}}{3\rho + \sigma} g^{\alpha\beta} - \tilde{\varphi}(\Omega)\left(g^{\alpha\gamma} g^{\beta\delta} D_{\gamma\delta} - \frac{\mathrm{E}}{3} g^{\alpha\beta} \right)\right], \tag{1.1}$$

where

$$\Omega = \sqrt{\frac{1}{\sigma}\left(Y - \frac{E^2}{3} \right)} \tag{1.2}$$

S. P. Timoshenko Institute of Mechanics, National Academy of Sciences of Ukraine, 3 Nesterova St., Kyiv, Ukraine 03057, e-mail: fract@inmech.kiev.ua. Translated from Prikladnaya Mekhanika, Vol. 48, No. 5, pp. 79–91, September–October 2012. Original article submitted December 6, 2010.

$$(E = g^{\alpha\beta} D_{\alpha\beta},\ Y = g^{\alpha\gamma} g^{\beta\delta} D_{\alpha\beta} D_{\gamma\delta}). \tag{1.3}$$

The constants ρ and σ may be expressed in terms of the Lame constants [13].

Following [12], we introduce the constant $\upsilon > 0$ and define the function $\tilde{\varphi}(\Omega)$ as

$$\tilde{\varphi}(\Omega)\big|_{\Omega \le \upsilon} = 0, \quad \tilde{\varphi}(\Omega)\big|_{\Omega > \upsilon} = \frac{\Omega - \upsilon + p - \sqrt[3]{\sqrt{q^3 + r^2} - r} + \sqrt[3]{\sqrt{q^3 + r^2} + r}}{\Omega} \tag{1.4}$$

$$\left(p = \frac{b}{3c},\ q = p^2 + \frac{1}{3c},\ r = p^3 - \frac{1}{2c}(\Omega - \upsilon + p) \right), \tag{1.5}$$

where υ, b, and c are assumed known.

1.2. Nonlinearity Criterion. Considering (1.4), we conclude that relationship (1.1) between the tensors ***S*** and ***D*** is linear if $\Omega \le \upsilon$ and nonlinear if $\Omega > \upsilon$, i.e.,

$$\Omega = \upsilon. \tag{1.6}$$

Introducing a variable ω, we represent the components of the strain tensor ***D*** as

$$D_{\varepsilon\zeta} = \omega g_{\varepsilon\zeta}. \tag{1.7}$$

Substituting (1.7) into (1.3) yields

$$E = 3\omega, \quad Y = 3\omega^2, \tag{1.8}$$

where

$$Y - E^2 / 3 = 0. \tag{1.9}$$

This means that, according to (1.2), the components of the tensor ***D*** given by (1.7) cannot satisfy criterion (1.6).

2. Generalities. Let us introduce an orthogonal coordinate system x^1, x^2, x^3 for which the components of the metric tensor ***g*** are given by

$$g^{\varepsilon\varsigma} = \begin{cases} 1, & \varepsilon = \varsigma, \\ 0, & \varepsilon \ne \varsigma. \end{cases} \tag{2.1}$$

2.1. Basic Equations. Let us derive the basic equations for the components of the displacement vector ***u***. The components of the strain tensor ***D*** and the components of the displacement vector ***u*** are related as follows [9]:

$$D_{\varepsilon\varsigma} = \frac{\partial u_\varepsilon}{\partial x^\varsigma}(\varepsilon, \varsigma), \tag{2.2}$$

where symmetrization over the indices ε and ς is assumed.

Using (1.3), (2.1), and (2.2), we get

$$E = \sum_{\beta=1}^{3} \frac{\partial u_\beta}{\partial x^\beta}, \quad Y = \frac{1}{4} \sum_{\gamma=1}^{3} \sum_{\delta=1}^{3} \left(\frac{\partial u_\gamma}{\partial x^\delta} + \frac{\partial u_\delta}{\partial x^\gamma} \right) \left(\frac{\partial u_\gamma}{\partial x^\delta} + \frac{\partial u_\delta}{\partial x^\gamma} \right). \tag{2.3}$$

With (2.2), Eqs. (1.1) become:

$$S^{\alpha\beta} = \frac{1}{\sigma} \left\{ \frac{1}{2} g^{\alpha\gamma} g^{\beta\delta} \left(\frac{\partial u_\gamma}{\partial x^\delta} + \frac{\partial u_\delta}{\partial x^\gamma} \right) - \frac{\rho E}{3\rho + \sigma} g^{\alpha\beta} \right.$$

$$-\tilde{\varphi}(\Omega)\left[\frac{1}{2}g^{\alpha\gamma}g^{\beta\delta}\left(\frac{\partial u_\gamma}{\partial x^\delta}+\frac{\partial u_\delta}{\partial x^\gamma}\right)-\frac{E}{3}g^{\alpha\beta}\right]\Bigg\}. \tag{2.4}$$

Let us consider a generalized plane stress state:

$$S^{\alpha\beta}=S^{\alpha\beta}(x^1,x^2)\quad(\alpha=1,2,\ \beta=1,2), \tag{2.5}$$

$$S^{\alpha\beta}=0\quad(\alpha=1,2,\ \beta=3,\ \alpha=3,\ \beta=1,2,\ \alpha=3,\ \beta=3). \tag{2.6}$$

Considering that $\tilde{\varphi}(\Omega)\neq 1$and using formula (2.1) and the first four equalities in (2.6), we reduce Eq. (2.4) to the form

$$\frac{\partial u_\gamma}{\partial x^\delta}+\frac{\partial u_\delta}{\partial x^\gamma}=0\quad(\gamma=1,2,\ \delta=3,\ \gamma=3,\ \delta=1,2). \tag{2.7}$$

Using the last equality in (2.6), the first formula in (2.3), and Eqs. (2.1) and (2.4), we get

$$\frac{\partial u_3}{\partial x^3}=\frac{3\rho+\sigma}{2\rho+\sigma}\left[\frac{\rho}{3\rho+\sigma}\left(\frac{\partial u_1}{\partial x^1}+\frac{\partial u_2}{\partial x^2}\right)+\frac{1}{3}\tilde{\varphi}(\Omega)\left(2\frac{\partial u_3}{\partial x^3}-\frac{\partial u_1}{\partial x^1}-\frac{\partial u_2}{\partial x^2}\right)\right]. \tag{2.8}$$

Let

$$\underline{T}^{11}=\frac{2}{3}\tilde{\varphi}(\Omega)\left[(3\rho+2\sigma)\frac{\partial u_1}{\partial x^1}-(3\rho+\sigma)\frac{\partial u_2}{\partial x^2}-\sigma\frac{\partial u_3}{\partial x^3}\right],$$

$$\underline{T}^{12}=(2\rho+\sigma)\tilde{\varphi}(\Omega)\left(\frac{\partial u_1}{\partial x^2}+\frac{\partial u_2}{\partial x^1}\right),\quad \underline{T}^{21}=(2\rho+\sigma)\tilde{\varphi}(\Omega)\left(\frac{\partial u_2}{\partial x^1}+\frac{\partial u_1}{\partial x^2}\right),$$

$$\underline{T}^{22}=\frac{2}{3}\tilde{\varphi}(\Omega)\left[(3\rho+2\sigma)\frac{\partial u_2}{\partial x^2}-(3\rho+\sigma)\frac{\partial u_1}{\partial x^1}-\sigma\frac{\partial u_3}{\partial x^3}\right]. \tag{2.9}$$

With (2.5) and (2.6), the equilibrium equations for the components of the stress tensor $\boldsymbol{S}$ [9] reduce to

$$\frac{\partial S^{11}}{\partial x^1}+\frac{\partial S^{12}}{\partial x^2}=0,\quad \frac{\partial S^{21}}{\partial x^1}+\frac{\partial S^{22}}{\partial x^2}=0. \tag{2.10}$$

Assume that the constants ρ and σ are independent of the coordinates x^1 and x^2.
Using (2.1), (2.3), (2.4), (2.8), and (2.9), we reduce Eqs. (2.10) to

$$2(\rho+\sigma)\frac{\partial^2 u_1}{\partial x^1\partial x^1}+\sigma\frac{\partial^2 u_2}{\partial x^1\partial x^2}+(2\rho+\sigma)\frac{\partial^2 u_1}{\partial x^2\partial x^2}=\underline{Q}^1,$$

$$(2\rho+\sigma)\frac{\partial^2 u_2}{\partial x^1\partial x^1}+\sigma\frac{\partial^2 u_1}{\partial x^1\partial x^2}+2(\rho+\sigma)\frac{\partial^2 u_2}{\partial x^2\partial x^2}=\underline{Q}^2 \tag{2.11}$$

$$\left(\underline{Q}^1=\frac{\partial\underline{T}^{11}}{\partial x^1}+\frac{\partial\underline{T}^{12}}{\partial x^2},\ \ \underline{Q}^2=\frac{\partial\underline{T}^{21}}{\partial x^1}+\frac{\partial\underline{T}^{22}}{\partial x^2}\right). \tag{2.12}$$

Thus, we have derived second-order partial differential equations for u_1 and u_2 with respect to x^1 and x^2.

Let us specify a stress vector $\boldsymbol{P}$ on the surfaces of the body, crack, and cut (with a unit outward normal $\boldsymbol{n}$).
According to (2.6), the boundary conditions for the components of the stress tensor $\boldsymbol{S}$ [9] are

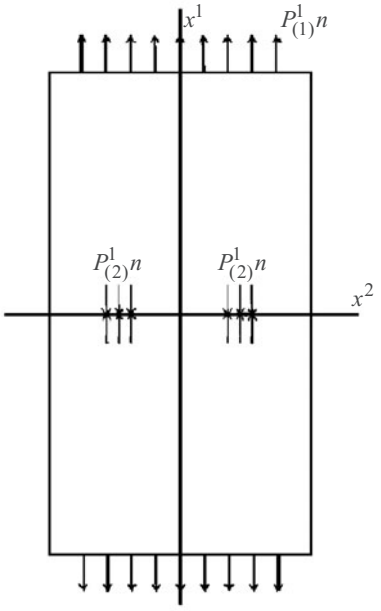

Fig. 1

$$S^{11}n_1 + S^{12}n_2 = P^1, \quad S^{21}n_1 + S^{22}n_2 = P^2. \tag{2.13}$$

Using the notation

$$2\sigma(2\rho + \sigma)P^\alpha \equiv \underline{P}^\alpha \quad (\alpha = 1, 2), \tag{2.14}$$

conditions (2.13), Eqs. (2.4), equalities (2.1), the first formula in (2.3), and formulas (2.8), and (2.9), we get

$$2\left[(\rho+\sigma)\frac{\partial u_1}{\partial x^1} - \rho\frac{\partial u_2}{\partial x^2}\right]n_1 + (2\rho+\sigma)\left(\frac{\partial u_1}{\partial x^2} + \frac{\partial u_2}{\partial x^1}\right)n_2 = \underline{P}^1 + \underline{R}^1,$$

$$(2\rho+\sigma)\left(\frac{\partial u_2}{\partial x^1} + \frac{\partial u_1}{\partial x^2}\right)n_1 + 2\left[(\rho+\sigma)\frac{\partial u_2}{\partial x^2} - \rho\frac{\partial u_1}{\partial x^1}\right]n_2 = \underline{P}^2 + \underline{R}^2 \tag{2.15}$$

$$(\underline{R}^1 = \underline{T}^{11}n_1 + \underline{T}^{12}n_2, \quad \underline{R}^2 = \underline{T}^{21}n_1 + \underline{T}^{22}n_2). \tag{2.16}$$

Thus, we have derived first-order partial differential equations for u_1 and u_2 with respect to x^1 and x^2.

Equations (2.11) and (2.15) can be integrated by Il'yushin's method of successive approximations [3]. The quantities $\underline{Q}^1, \underline{Q}^2$ and $\underline{R}^1, \underline{R}^2$ should be equated to zero in the first approximation. In the subsequent approximations, they should be calculated from the previous approximation. If $\tilde{\varphi}(\Omega) = 0$, then $\underline{Q}^1, \underline{Q}^2$ and $\underline{R}^1, \underline{R}^2$ are equal to zero (according to (2.9), (2.12), and (2.16)), and integrating Eqs. (2.11) and (2.15) yields the solution of the linear elastic boundary-value problem as the first approximation.

2.2. Boundary-Value Problem Formulation. Consider a thin rectangular body with a central crack (Fig. 1). The axes of symmetry of the body are aligned with the x^1- and x^2-axes. As the body is stretched along the x^1-axis, a narrow zone (fracture process zone) occurs near each crack tip. This zone cannot be described by the above equations. Let us model this zone by a cut with uniformly distributed stresses applied to its faces. These stresses can be determined by solving a boundary-value problem.

We specify the components P^1 and P^2 on the surfaces of the body, crack, and cut, symmetrically about the x^1- and x^2-axes. Then it is sufficient to analyze a quarter of the body. We choose the quarter located in the first quadrant (Fig. 1).

On the upper surface of this part of the body, $n_1 = 1$, $n_2 = 0$, and Eqs. (2.15) have the form

$$2\left[(\rho+\sigma)\frac{\partial u_1}{\partial x^1}-\rho\frac{\partial u_2}{\partial x^2}\right]=\underline{P}^1+\underline{R}^1,$$

$$(2\rho+\sigma)\left(\frac{\partial u_2}{\partial x^1}+\frac{\partial u_1}{\partial x^2}\right)=\underline{P}^2+\underline{R}^2, \tag{2.17}$$

where $\underline{R}^1=\underline{T}^{11}$, $\underline{R}^2=\underline{T}^{21}$ according to (2.16).

On the lateral surface of this part of the body, $n_1=0, n_2=1$ and Eqs. (2.15) have the form

$$(2\rho+\sigma)\left(\frac{\partial u_1}{\partial x^2}+\frac{\partial u_2}{\partial x^1}\right)=\underline{P}^1+\underline{R}^1,$$

$$2\left[(\rho+\sigma)\frac{\partial u_2}{\partial x^2}-\rho\frac{\partial u_1}{\partial x^1}\right]=\underline{P}^2+\underline{R}^2, \tag{2.18}$$

where $\underline{R}^1=\underline{T}^{12}$, $\underline{R}^2=\underline{T}^{22}$ according to (2.16).

On the upper face of the crack, $-n_1=1, n_2=0$ and Eqs. (2.15) have the form

$$-2\left[(\rho+\sigma)\frac{\partial u_1}{\partial x^1}-\rho\frac{\partial u_2}{\partial x^2}\right]=\underline{P}^1+\underline{R}^1,$$

$$-(2\rho+\sigma)\left(\frac{\partial u_2}{\partial x^1}+\frac{\partial u_1}{\partial x^2}\right)=\underline{P}^2+\underline{R}^2, \tag{2.19}$$

where $-\underline{R}^1=\underline{T}^{11}$, $-\underline{R}^2=\underline{T}^{21}$ according to (2.16).

Since there is symmetry about the x^1- and x^2-axes, we have

$$u_1(x^1,-x^2)-u_1(x^1,+x^2)=0,\ \ u_2(x^1,-x^2)+u_2(x^1,+x^2)=0,$$

$$u_1(-x^1,x^2)+u_1(+x^1,x^2)=0,\ \ u_2(-x^1,x^2)-u_2(+x^1,x^2)=0. \tag{2.20}$$

Moreover, by symmetry about the x^2-axis, we have

$$u_1=0 \tag{2.21}$$

at the tip of the cut.

Let us derive an equation containing u_2. To this end, we choose an arbitrary point (a^1, a^2) near the cut tip. Let all partial derivatives (up to the second order) of u_2 with respect to x^1 and x^2 exist at this point. The coordinates of the cut tip are $a^1+\varepsilon^1$ and $a^2+\varepsilon^2$.

Let us expand u_2 into a multiple Taylor series in powers of ε^1 and ε^2:

$$u_2=u_2(a^1,a^2)+\sum_{\beta=1}^{2}\left.\frac{\partial u_2}{\partial x^\beta}\right|_{(a^1,a^2)}\varepsilon^\beta+\frac{1}{2}\sum_{\beta=1}^{2}\sum_{\gamma=1}^{2}\left.\frac{\partial^2 u_2}{\partial x^\beta\,\partial x^\gamma}\right|_{(a^1,a^2)}\varepsilon^\beta\varepsilon^\gamma, \tag{2.22}$$

whence

$$-u_2+u_2(a^1,a^2)+\left.\frac{\partial u_2}{\partial x^1}\right|_{(a^1,a^2)}\varepsilon^1+\left.\frac{\partial u_2}{\partial x^2}\right|_{(a^1,a^2)}\varepsilon^2$$

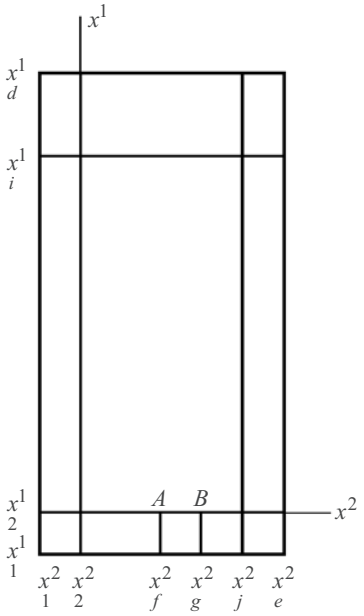

Fig. 2

$$+\frac{1}{2}\left(\left.\frac{\partial^2 u_2}{\partial x^1 \partial x^1}\right|_{(a^1,a^2)} \varepsilon^1\varepsilon^1 + 2\left.\frac{\partial^2 u_2}{\partial x^1 \partial x^2}\right|_{(a^1,a^2)} \varepsilon^1\varepsilon^2 + \left.\frac{\partial^2 u_2}{\partial x^2 \partial x^2}\right|_{(a^1,a^2)} \varepsilon^2\varepsilon^2\right) = 0. \tag{2.23}$$

Note that Eqs. (2.11), (2.17)–(2.21), and (2.23) are the governing equations for u_1 and u_2.

2.3. Transformation of the Governing Equations. We introduce a coordinate mesh with a spacing h (Fig. 2):

$$x^1_i = (i-2)h \qquad (i = 1, 2, \ldots, d),$$

$$x^2_j = (j-2)h \qquad (j = 1, 2, \ldots, e). \tag{2.24}$$

Let the tips of the crack and the cut be points A and B with coordinates x^1_2, x^2_f and x^1_2, x^2_g, respectively.

Denote

$$u_1(x^1_i, x^2_j) \equiv y_s, \quad u_2(x^1_i, x^2_j) \equiv y_t \tag{2.25}$$

$$\left(s = 2[(i-1)e + j - g] + 1,\ t = 2[(i-1)e + j - g] + 2\right). \tag{2.26}$$

Expressing the partial derivatives of u_1 and u_2 with respect to x^1 and x^2 in terms of finite differences (using formulas (2.24)–(2.26)), using Eqs. (2.11), (2.17)–(2.21), and (2.23), and setting $-\varepsilon^1 = \varepsilon^2 = h$, we obtain n linear algebraic equations with unknowns $y_1, y_2, \ldots, y_n$:

$$A_{ss}y_s + A_{ss+2e}y_{s+2e} + A_{ss-2e}y_{s-2e} + A_{ss+2}y_{s+2} + A_{ss-2}y_{s-2}$$
$$+A_{st+2(e+1)}y_{t+2(e+1)} + A_{st+2(e-1)}y_{t+2(e-1)} + A_{st-2(e-1)}y_{t-2(e-1)} + A_{st-2(e+1)}y_{t-2(e+1)} \approx B_s,$$
$$A_{tt}y_t + A_{tt+2e}y_{t+2e} + A_{tt-2e}y_{t-2e} + A_{tt+2}y_{t+2} + A_{tt-2}y_{t-2}$$
$$+A_{ts+2(e+1)}y_{s+2(e+1)} + A_{ts+2(e-1)}y_{s+2(e-1)} + A_{ts-2(e-1)}y_{s-2(e-1)} + A_{ts-2(e+1)}y_{s-2(e+1)} \approx B_t$$

$$(i=2,\ j=g+1,\dots,e-1,\ i=3,\dots,d-1,\ j=2,\dots,e-1),$$

$$A_{ss}y_s + A_{ss-2e}y_{s-2e} + A_{ss-4e}y_{s-4e} + A_{ss-6e}y_{s-6e}$$

$$+A_{ss-2}y_{s-2} + A_{ss-4}y_{s-4} + A_{ss-6}y_{s-6} + A_{st}y_t + A_{st-2}y_{t-2} + A_{st-4}y_{t-4}$$

$$+A_{st-2e}y_{t-2e} + A_{st-2(e+1)}y_{t-2(e+1)} + A_{st-2(e+2)}y_{t-2(e+2)}$$

$$+A_{st-4e}y_{t-4e} + A_{st-2(2e+1)}y_{t-2(2e+1)} + A_{st-4(e+1)}y_{t-4(e+1)} \approx B_s,$$

$$A_{tt}y_t + A_{tt-2e}y_{t-2e} + A_{tt-4e}y_{t-4e} + A_{tt-6e}y_{t-6e}$$

$$+A_{tt-2}y_{t-2} + A_{tt-4}y_{t-4} + A_{tt-6}y_{t-6} + A_{ts}y_s + A_{ts-2}y_{s-2} + A_{ts-4}y_{s-4}$$

$$+A_{ts-2e}y_{s-2e} + A_{ts-2(e+1)}y_{s-2(e+1)} + A_{ts-2(e+2)}y_{s-2(e+2)}$$

$$+A_{ts-4e}y_{s-4e} + A_{ts-2(2e+1)}y_{s-2(2e+1)} + A_{ts-4(e+1)}y_{s-4(e+1)} \approx B_t \quad (i=d,\ j=e),$$

$$A_{ss}y_s + A_{ss-2e}y_{s-2e} + A_{ss-4e}y_{s-4e} + A_{st+2}y_{t+2} + A_{st-2}y_{t-2} \approx B_s,$$

$$A_{tt}y_t + A_{tt-2e}y_{t-2e} + A_{tt-4e}y_{t-4e} + A_{ts+2}y_{s+2} + A_{ts-2}y_{s-2} \approx B_t \quad (i=d,\ j=2,\dots,e-1),$$

$$A_{ss}y_s + A_{ss-2}y_{s-2} + A_{ss-4}y_{s-4} + A_{st+2e}y_{t+2e} + A_{st-2e}y_{t-2e} \approx B_s,$$

$$A_{tt}y_t + A_{tt-2}y_{t-2} + A_{tt-4}y_{t-4} + A_{ts+2e}y_{s+2e} + A_{ts-2e}y_{s-2e} \approx B_t \quad (i=2,\dots,d-1,\ j=e),$$

$$A_{ss}y_s + A_{ss+2e}y_{s+2e} + A_{ss+4e}y_{s+4e} + A_{st+2}y_{t+2} + A_{st-2}y_{t-2} \approx B_s,$$

$$A_{tt}y_t + A_{tt+2e}y_{t+2e} + A_{tt+4e}y_{t+4e} + A_{ts+2}y_{s+2} + A_{ts-2}y_{s-2} \approx B_t \quad (i=2,\ j=2,\dots,g-1),$$

$$A_{s-2s-2}y_{s-2} + A_{s-2s+2}y_{s+2} = B_{s-2}, \quad A_{t-2t-2}y_{t-2} + A_{t-2t+2}y_{t+2} = B_{t-2} \quad (i=2,\dots,d,\ j=2),$$

$$A_{s-2es-2e}y_{s-2e} + A_{s-2es+2e}y_{s+2e} = B_{s-2e}, \quad A_{t-2et-2e}y_{t-2e} + A_{t-2et+2e}y_{t+2e} = B_{t-2e}$$

$$(i=2,\ j=g,\dots,e),$$

$$A_{ss}y_s = B_s, \quad A_{tt}y_t + A_{tt-4}y_{t-4} + A_{tt-2}y_{t-2}$$

$$+A_{tt+2(e-1)}y_{t+2(e-1)} + A_{tt+2e}y_{t+2e} + A_{tt+4(e-1)}y_{t+4(e-1)} + A_{tt+4e}y_{t+4e} \approx B_t \quad (i=2,\ j=g) \tag{2.27}$$

$$(-A_{ss} = 8(4\rho+3\sigma),\ A_{ss+2e} = 8(\rho+\sigma),$$

$$A_{ss-2e} = 8(\rho+\sigma), \quad A_{ss+2} = 4(2\rho+\sigma), \quad A_{ss-2} = 4(2\rho+\sigma),$$

$$A_{st+2(e+1)} = \sigma, \quad -A_{st+2(e-1)} = \sigma, \quad -A_{st-2(e-1)} = \sigma, \quad A_{st-2(e+1)} = \sigma, \quad B_s = 4h^2 \underset{\sim}{Q}{}^1_{ij}(x^1, x^2),$$

$$-A_{tt} = 8(4\rho+3\sigma),\ A_{tt+2e} = 4(2\rho+\sigma),\ A_{tt-2e} = 4(2\rho+\sigma),$$

$$A_{tt+2} = 8(\rho+\sigma), \quad A_{tt-2} = 8(\rho+\sigma),$$

$$A_{ts+2(e+1)} = \sigma, \quad -A_{ts+2(e-1)} = \sigma, \quad -A_{ts-2(e-1)} = \sigma, \quad A_{ts-2(e+1)} = \sigma, \quad B_t = 4h^2 \underset{\sim}{Q}{}^2_{ij}(x^1, x^2)$$

$$(i=2,\ j=g+1,\dots,e-1,\ i=3,\dots,d-1,\ j=2,\dots,e-1),$$

$$A_{ss} = 8(4\rho+3\sigma), \quad -A_{ss-2e} = 40(\rho+\sigma), \quad A_{ss-4e} = 32(\rho+\sigma), \ -A_{ss-6e} = 8(\rho+\sigma),$$

$$-A_{ss-2} = 20(2\rho+\sigma), \quad A_{ss-4} = 16(2\rho+\sigma), \quad -A_{ss-6} = 4(2\rho+\sigma),$$

$$A_{st} = 9\sigma, \quad -A_{st-2} = 12\sigma, \quad A_{st-4} = 3\sigma, \quad -A_{st-2e} = 12\sigma, \quad A_{st-2(e+1)} = 16\sigma,$$

$$-A_{st-2(e+2)}=4\sigma,\quad A_{st-4e}=3\sigma,\quad -A_{st-2(2e+1)}=4\sigma,\quad A_{st-4(e+1)}=\sigma,\quad B_s=4h^2\underline{Q}^1_i(x^1_i,x^2_j),$$

$$A_{tt}=8(4\rho+3\sigma),\quad -A_{tt-2e}=20(2\rho+\sigma),\quad A_{tt-4e}=16(2\rho+\sigma),\quad -A_{tt-6e}=4(2\rho+\sigma),$$

$$-A_{tt-2}=40(\rho+\sigma),\quad A_{tt-4}=32(\rho+\sigma),\quad -A_{tt-6}=8(\rho+\sigma),\quad A_{ts}=9\sigma,$$

$$-A_{ts-2}=12\sigma,\quad A_{ts-4}=3\sigma,\quad -A_{ts-2e}=12\sigma,\quad A_{ts-2(e+1)}=16\sigma,\quad -A_{ts-2(e+2)}=4\sigma,$$

$$A_{ts-4e}=3\sigma,\quad -A_{ts-2(2e+1)}=4\sigma,\quad A_{ts-4(e+1)}=\sigma,\quad B_t=4h^2\underline{Q}^2_i(x^1_i,x^2_j)\quad (i=d,\ j=e),$$

$$A_{ss}=6(\rho+\sigma),\quad -A_{ss-2e}=8(\rho+\sigma),\quad A_{ss-4e}=2(\rho+\sigma),\quad -A_{st+2}=2\rho,\ A_{st-2}=2\rho,$$

$$B_s=2h\left[\underline{P}^1_i(x^1_i,x^2_j)+\underline{R}^1_i(x^1_i,x^2_j)\right],$$

$$A_{tt}=3(2\rho+\sigma),\quad -A_{tt-2e}=4(2\rho+\sigma),\quad A_{tt-4e}=2\rho+\sigma,\quad A_{ts+2}=2\rho+\sigma,\quad -A_{ts-2}=2\rho+\sigma,$$

$$B_t=2h\left[\underline{P}^2_i(x^1_i,x^2_j)+\underline{R}^2_i(x^1_i,x^2_j)\right]\quad (i=d,\ j=2,\dots,\ e-1),$$

$$A_{ss}=3(2\rho+\sigma),\quad -A_{ss-2}=4(2\rho+\sigma),\quad A_{ss-4}=2\rho+\sigma,\quad A_{st+2e}=2\rho+\sigma,\quad -A_{st-2e}=2\rho+\sigma,$$

$$B_s=2h\left[\underline{P}^1_i(x^1_i,x^2_j)+\underline{R}^1_i(x^1_i,x^2_j)\right],$$

$$A_{tt}=6(\rho+\sigma),\quad -A_{tt-2}=8(\rho+\sigma),\quad A_{tt-4}=2(\rho+\sigma),\quad -A_{ts+2e}=2\rho,\quad A_{ts-2e}=2\rho,$$

$$B_t=2h\left[\underline{P}^2_i(x^1_i,x^2_j)+\underline{R}^2_i(x^1_i,x^2_j)\right]\quad (i=2,\dots,d-1,\ j=e),$$

$$A_{ss}=6(\rho+\sigma),\quad -A_{ss+2e}=8(\rho+\sigma),\quad A_{ss+4e}=2(\rho+\sigma),\quad A_{st+2}=2\rho,\quad -A_{st-2}=2\rho,$$

$$B_s=2h\left[\underline{P}^1_i(x^1_i,x^2_j)+\underline{R}^1_i(x^1_i,x^2_j)\right],$$

$$A_{tt}=3(2\rho+\sigma),\quad -A_{tt+2e}=4(2\rho+\sigma),\quad A_{tt+4e}=2\rho+\sigma,\quad -A_{ts+2}=2\rho+\sigma,\quad A_{ts-2}=2\rho+\sigma,$$

$$B_t=2h\left[\underline{P}^2_i(x^1_i,x^2_j)+\underline{R}^2_i(x^1_i,x^2_j)\right]\quad (i=2,\ j=2,\dots,\ g-1),$$

$$A_{s-2s-2}=1,\quad -A_{s-2s+2}=1,\quad B_{s-2}=0,\quad A_{t-2t-2}=1,\quad A_{t-2t+2}=1,\quad B_{t-2}=0$$

$$(i=2,\dots,d,\ j=2),$$

$$A_{s-2es-2e}=1,\quad A_{s-2es+2e}=1,\quad B_{s-2e}=0,\quad A_{t-2et-2e}=1,\quad -A_{t-2et+2e}=1,\quad B_{t-2e}=0$$

$$(i=2,\ j=g,\dots,e),$$

$$A_{ss}=1,\quad B_s=0,\quad -A_{tt}=3,\quad -A_{tt-4}=1,\quad A_{tt-2}=4,$$

$$-A_{tt+2(e-1)}=4,\quad A_{tt+2e}=4,\quad A_{tt+4(e-1)}=1,\quad -A_{tt+4e}=1,\quad B_t=0$$

$$(i=2,\ j=g)).\qquad (2.28)$$

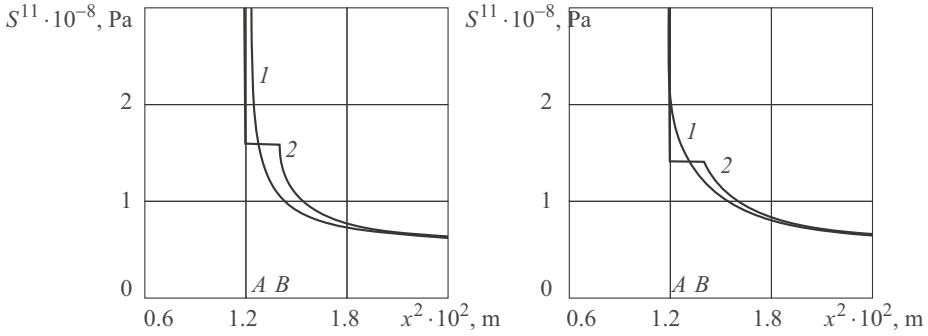

Fig. 3

Note that the quantities $\underline{Q}^1, \underline{Q}^2$ and $\underline{R}^1, \underline{R}^2$ should be expressed in terms of the unknowns $y_1, \ldots, y_n$ by representing the first-order partial derivatives of u_1 and u_2 with respect to x^1 and x^2 in terms of finite differences (using (2.20) and (2.24)–(2.26)). To solve Eqs. (2.27), we use the modified Gaussian elimination method [12].

3. Numerical Example. Let us study how the fracture process zone affects the size and shape of the nonlinear zone in the case of a generalized plane stress state. To this end, we will examine the deformation of a nonlinear elastic body with a crack and compare it with the behavior of a linear elastic body. Let the lengths of the crack and cut be the same in both bodies.

3.1. Solution of the Boundary-Value Problem. To solve the problem, we will use the following input data from [13]:

$$\rho = 0.046\cdot 10^{-10}\ \text{Pa}^{-1}, \qquad \sigma = 0.222\cdot 10^{-10}\ \text{Pa}^{-1},$$

$$\upsilon = 3.25\cdot 10^{2}\ \text{Pa}^{1/2}, \quad b = 0.1964347\cdot 10^{-2}\ \text{Pa}^{-1/2}, \quad c = 0.5632820\cdot 10^{-4}\ \text{Pa}^{-1},$$

$$h = 0.02\cdot 10^{-2}\ \text{m}, \quad d = 30, \quad e = 15, \quad f = 6, \quad g = 7.$$

Using the second formula in (2.24), we find the lengths of the crack and the cut, respectively: $x^2_f - x^2_2 = (f-2)h = 1.20\cdot 10^{-2}$ m; $x^2_g - x^2_f = (g-f)h = 0.20\cdot 10^{-2}$ m.

Note that only P^1 (on the upper surfaces of the body and cut) is nonzero and independent of x^2:

$$P^1(x^1_d, x^2_j) = P^1_{(1)} \qquad (j = 2, \ldots, e-1),$$

$$P^1(x^1_2, x^2_j) = P^1_{(2)} \qquad (j = f, \ldots, g-1).$$

The boundary-value problem is solved assuming that the component S^{11} at the tip of the cut has the same value as at all other points on its upper face:

$$S^{11}(x^1_2, x^2_g) = |P^1_{(2)}|. \tag{3.1}$$

Expressing the partial derivatives of u_1 and u_2 with respect to x^1 and x^2, respectively, in terms of central differences (using (2.24)–(2.26)) and using Eqs. (2.4), the first formula in (2.3), the first formula in (2.9), and expression (2.8), we obtain

$$S^{11}(x^1_2, x^2_j) \approx \frac{1}{2\sigma(2\rho+\sigma)}\left\{\frac{1}{h}\left[(\rho+\sigma)\left(y_{2(2e+j-g)+1} - y_{2(j-g)+1}\right)\right.\right.$$

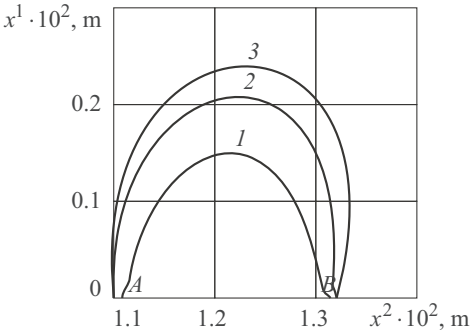

Fig. 4

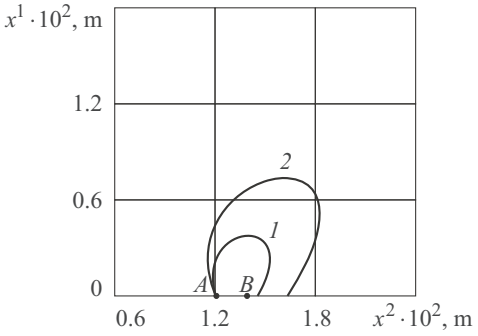

Fig. 5

$$-\rho\left(y_{2(e+j-g)+4} - y_{2(e+j-g)}\right)\Big] - \underline{T}^{11}\left(\underset{2}{x^1}, \underset{j}{x^2}\right)\Big\} \quad (j = g, \ldots, e-1). \tag{3.2}$$

We examine two cases for linear and nonlinear elastic bodies: absence and presence of the fracture process zone.

The values of $y_1, \ldots, y_n$ are determined from Eqs. (2.27) using 15 approximations (and formulas (2.28) with notation (2.14)). The quantities $\underline{Q}^1, \underline{Q}^2$ and $\underline{R}^1, \underline{R}^2$ are equal to zero in the first approximation. In the subsequent approximations, they are calculated (using (2.9), (1.4), (1.5), (2.3), (2.7), (2.8), (2.25), and (2.26)) from the values of $y_1, \ldots, y_n$ found in the previous approximation.

If the fracture process zone is present, the solution of the boundary-value problem is found in several iterations. The value of $P^1_{(2)}$ is initially specified and then is corrected (until condition (3.1) is satisfied) using the value of S^{11} at the cut tip found by formula (3.2) from the values of $y_{4e+1}, y_1, y_{2(e+2)}, y_{2e}$ and the corresponding value of $\underline{T}^{11}$. We use $P^1_{(1)} = 5.00 \cdot 10^7$ Pa. When the fracture process zone is present, $-P^1_{(2)} = 15.90 \cdot 10^7$ Pa for the linear elastic body and $-P^1_{(2)} = 14.14 \cdot 10^7$ Pa for the nonlinear elastic body.

3.2. Analysis of the Results. The value of S^{11} on the upper face of the cut $(S^{11}(\underset{2}{x^1}, \underset{j}{x^2}) = |P^1_{(2)}| \ (j = f, \ldots, g-1))$ in the linear elastic body is much greater than in the nonlinear elastic body.

The values of S^{11} ahead of the cut tip are determined by formula (3.2) from the values of $y_{2(2e+j-g)+1}$, $y_{2(j-g)+1}$, $y_{2(e+j-g)+4}$, $y_{2(e+j-g)}$ and the corresponding values of $\underline{T}^{11}$. Figures 3*a* and 3*b* show S^{11} as a function of x^2 for $x^1 = \underset{2}{x^1}$ for linear and nonlinear elastic bodies, respectively (curves *1* correspond to the absence of the fracture process zone and curves *2* to the presence of this zone).

With distance from the cut tip, the difference of the values of S^{11} for linear and nonlinear elastic bodies with fracture process zone first decreases becoming negative and then increases remaining negative. It is equal to $1.76 \cdot 10^7$ Pa at $x^2 = 1.40 \cdot 10^{-2}$ m, to $-0.74 \cdot 10^7$ Pa at $x^2 = 1.54 \cdot 10^{-2}$ m, and to $-0.73 \cdot 10^7$ Pa at $x^2 = 1.56 \cdot 10^{-2}$ m.

As expected, the difference between the values of $P^1_{(2)}$ for linear and nonlinear elastic bodies decreases with decreasing value of $P^1_{(1)}$. If $P^1_{(1)} = 4.00 \cdot 10^7$ Pa, then $-P^1_{(2)} = 12.72 \cdot 10^7$ Pa for the linear elastic body and $-P^1_{(2)} = 12.31 \cdot 10^7$ Pa for the nonlinear elastic body. This is because the nonlinear zone contracts with decreasing value of $P^1_{(1)}$.

In solving the boundary-value problem for the nonlinear body at several values of $P^1_{(1)}$, we discoverd points at which criterion (1.6) is satisfied, i.e., we identify the boundaries of the nonlinear zone. The length of the nonlinear zones along the x^2-axis equals $0.22 \cdot 10^{-2}$ m if $P^1_{(1)} \le 3.53 \cdot 10^7$ Pa and exceeds $0.22 \cdot 10^{-2}$ m if $P^1_{(1)} > 3.53 \cdot 10^7$ Pa.

Figures 4 and 5 illustrate the boundaries of the nonlinear zones for the values of $P^1_{(1)}$ satisfying the above conditions. Curves *1*, *2*, and *3* in Fig. 4 correspond to $P^1_{(1)} = -3.20 \cdot 10^7, -3.40 \cdot 10^7, -3.53 \cdot 10^7$ Pa, respectively, which, in turn, correspond to

$-P^1_{(2)} = 10.17 \cdot 10^7, 10.77 \cdot 10^7, 11.14 \cdot 10^7$ Pa. As is seen, the nonlinear zones substantially differ in both size and shape. Indeed, their lengths are equal along the x^2-axis and different along the x^1-axis. The height of these zones is equal to $0.14 \cdot 10^{-2}$ m (curve *1*), $0.20 \cdot 10^{-2}$ m (curve *2*), and $0.24 \cdot 10^{-2}$ m (curve *3*).

As the coordinate x^1 increases, the width of the first zone decreases, the width of the second zone does not change, and the width of the third zone first increases and then decreases. When $x^1 = 0.04 \cdot 10^{-2}$ m, the width is equal to $0.18 \cdot 10^{-2}$, $0.22 \cdot 10^{-2}$, $0.24 \cdot 10^{-2}$ m, respectively.

Curves *1* and *2* in Fig. 5 correspond to $P^1_{(1)} = -4.00 \cdot 10^7, -5.00 \cdot 10^7$ Pa, respectively, which, in turn, correspond to $-P^1_{(2)} = 12.31 \cdot 10^7, 14.14 \cdot 10^7$ Pa. These nonlinear zones are similar in shape but substantially different in size. For example, they extend to $0.36 \cdot 10^{-2}$ m (curve *1*) and $0.72 \cdot 10^{-2}$ m (curve *2*) along the x^1-axis and to $0.26 \cdot 10^{-2}$ and $0.44 \cdot 10^{-2}$ m along the x^2-axis.

Determining the boundaries of the nonlinear zone for $P^1_{(1)} = 4.00 \cdot 10^7, 5.00 \cdot 10^7$ Pa in the absence and presence of the fracture process zone shows that the latter has a weak effect on the size and shape of the former.

Conclusions. We have studied the deformation of a nonlinear elastic body with a central mode I crack. The fracture process zone occurring near each crack tips under tension has been modeled by a cut with some stresses applied to its faces. A generalized plane stress state has been considered. A boundary-value problem has been formulated (for the components of the displacement vector), and linear tensor constitutive equations have been used. By solving this boundary-value problem numerically, we have determined the effect of the fracture process zone on the size and shape of the nonlinear zone. At the initial stage of deformation, the length of the nonlinear zone changes weakly along the crack and changes substantially in the perpendicular direction with increasing external load, i.e., there is a significant change in the shape of the zone. With further increase in the load, the nonlinear zone grows considerably in both directions, but its shape remains almost the same.

REFERENCES

1. G. I. Barenblatt and G. P. Cherepanov, “On the finiteness of stresses at the [leading] edge of an arbitrary crack,” *J. Appl. Math. Mech*., **25**, No. 4, 1112–1115 (1961).
2. Yu. P. Zheltov and S. A. Khristianovich, ”Hydraulic fracturing of an oil-bearing bed,” *Izv. AN SSSR*, *OTN*, No. 5, 3–41 (1955).
3. A. A. Il’yushin, ”Some issues of plastic deformation theory,” *Prikl. Mat. Mekh*., **7**, No. 4, 245–272 (1943).
4. A. A. Kaminsky and D. A. Gavrilov, *Stress Rupture of Polymeric and Composite Materials with Cracks* [in Russian], Naukova Dumka, Kyiv (1992).
5. A. A. Kaminsky, G. I. Usikova, E. E. Kurchakov, E. A. Dmitrieva, and S. P. Doroshenko, ”Experimental study of the plastic zone near a crack tip,” *Probl. Mashinostr. Avtomatiz*., No. 6, 79–85 (1991).
6. A. A. Kaminsky, G. I. Usikova, and E. A. Dmitrieva, ”Experimental study of the distribution of plastic strains near a crack tip during static loading,” *Int. Appl*, *Mech*., **30**, No. 11, 892–897 (1994).
7. V. V. Panasyuk, *Limiting Equilibrium of Brittle Bodies with Cracks* [in Russian], Naukova Dumka, Kyiv (1968).
8. V. V. Panasyuk and M. P. Savruk, ”Modeling plastic bands in elastoplastic problems of fracture mechanics,” *Fiz.-Khim. Mekh. Mater*., No. 2, 49–68 (1992).
9. I. S. Sokol’nikov, *Tensor Analysis* [in Russian], Nauka, Moscow (1971).
10. A. N. Guz, “Incorrect results in fracture mechanics,” *Int. Appl. Mech*., **45**, No. 10, 1041–1051 (2009).
11. A. A. Kaminsky, “Subcritical crack growth in polymer composite materials,” in: G. P. Cherepanov (ed.), *Fracture: A Topical Encyclopedia of Current Knowledge*, Krieger, Malabar (1998), pp. 758–765.
12. A. A. Kaminsky, E. E. Kurchakov, and G. V. Gavrilov, ”Inflence of tension along a crack on the plastic zone in an anisotropic body,” *Int. Appl. Mech*., **46**, No. 6, 634–648 (2010).
13. A. A. Kaminsky and E. E. Kurchakov, ”Modeling the fracture process zone near a crack tip in a nonlinear elastic body,” *Int. Appl. Mech*., **47**, No. 6, 735–744 (2011).